ORIGINAL PAPER Open Access



Electroblowing of poly(vinylidene fluoride) fibres—effect of hydroxyapatite precursors

Júnio A. R. Pasqual^{1*}, Mikko Ritala² and Carla C. Schmitt³

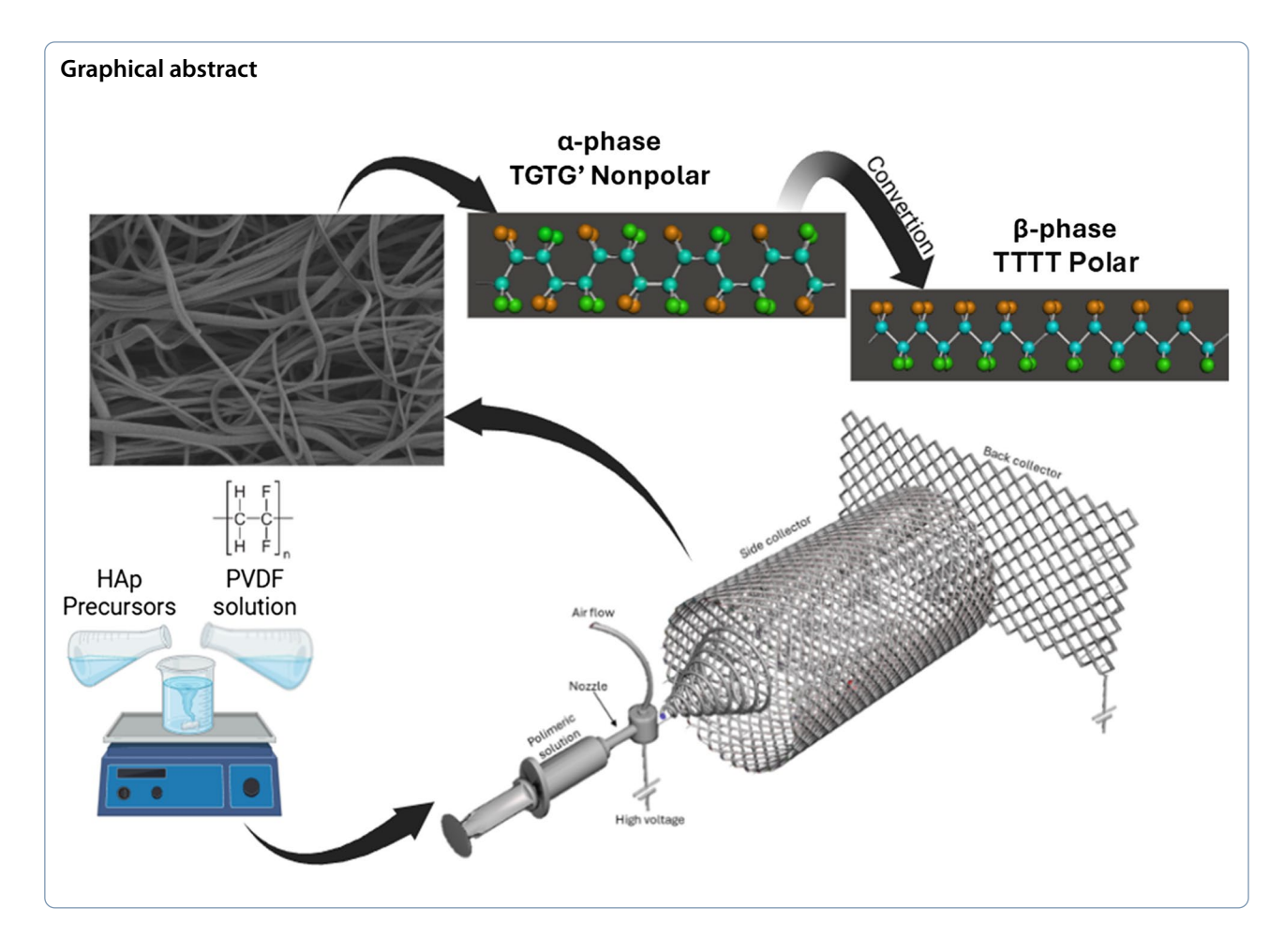
Abstract

Fibre production can be conducted using a variety of techniques, including electrospinning and electroblowing. These techniques require strict control of different parameters, such as the voltage, presence of fillers, viscosity, and airflow rate (for electroblowing). At the end of the process, fibres with different morphologies are obtained. Poly-1,1-difluoroethene (PVDF) is a polymer with excellent potential for fibre applications due to its properties, including good piezoelectricity, biocompatibility, and pyroelectricity. These attributes make PVDF suitable for biomedical applications. Other applications include conventional and hybrid nanogenerators, sensors, and potentially future green energy sources. To achieve a high production rate of fibres, parameter control must be sufficient to obtain fibres with the required characteristics at the spinning process. In this study, Ca(NO₃)₂·4H₂O and triethyl phosphate (TEP) were used as precursors at the hydroxyapatite (HAp) production within a polymeric solution to increase the PVDF fibre production rate and change morphology. The analysis techniques of X-ray diffraction, Fourier-transform infrared spectroscopy, Raman spectroscopy, scanning electron microscopy, transmission electron microscopy mechanical tensile test, and viscosity analysis were employed to observe the effect of the HAp precursor solution on the fibre's final properties. The addition of 5% and 10% of the solution containing these two precursors dissolved in ethanol (EtOH) increased the fibre diameter from 0.2 μm (without precursors) to 1.1 μm (5% of precursors) and 1.6 μm (10% of precursors). Additionally, the distribution of fibres on the collector became more uniform, suggesting a change in the fibre's electrical charge. These results demonstrate improved control of PVDF fibre production using a solution tailored for biomaterial purposes.

Keywords Fibres, Electroblowing, PVDF, HAp precursors

*Correspondence: Júnio A. R. Pasqual junio.pasqual@usp.br Full list of author information is available at the end of the article





Introduction

Spinning is a widely used method to make fibres with different morphologies and properties (Harshal Gade SNGGCDHR 2021; Sun et al. 2024). One of the most well-known techniques to produce fibres is electrospinning (Elnabawy et al. 2023; Purushothaman et al. 2023). This method is popular due to its low cost and rapid spinning capabilities (Li et al. 2021). However, there are other techniques to make polymer fibres, including thermalinduced phase separation, drawing, template synthesis, solution blow spinning, and electroblowing (Elnabawy et al. 2023; Li et al. 2021; Paajanen et al. 2023; Holopainen and Ritala 2016; Wang et al. 2018). Electroblowing, in particular, stands out for its speed, exceeding that of electrospinning (Demina et al. 2022). Besides high voltage, it uses airflow as a key parameter, which enhances fibre production compared to electrospinning (Elnabawy et al. 2023). This airflow increases the collector area for fibre deposition during spinning, allowing for the creation of a continuous and extensive fibre blanket.

A good spinning process for fibre production using the most common techniques, including electrospinning and electroblowing, requires meticulous control over multiple parameters beyond just airflow to ensure the quality of the product (Demina et al. 2022). The need for this control is the main focus of several studies on fibre production where the solvent, fillers, and the type of polymer can be changed (Sun et al. 2024; Purushothaman et al. 2023; Demina et al. 2022; Luchese et al. 2024). Alternatively, these parameters can be modified to find the best processing conditions to produce high-quality fibres (Elnabawy et al. 2023; Li et al. 2021; Demina et al. 2022; He et al. 2021). Each technique has specific conditions, but in all cases, especially electroblowing and electrospinning, the recipe, voltage, solution viscosity, solution feed rate, percentage of solvent, and rate of solvent evaporation need to be controlled during spinning (Paajanen et al. 2023; Holopainen and Ritala 2016; Demina et al. 2022). Therefore, the parameter values and type of material, including fillers, will vary for each spun polymer (Li et al. 2021; Demina et al. 2022). Attention to effective spinning processes has led to the identification and study of suitable materials, such as poly(vinylidene fluoride) (PVDF), for specific properties

that make them ideal for certain applications (Kujawa et al. 2024; Concha et al. 2024; Mokhtari et al. 2025; Bernard et al. 2018).

In the case of PVDF, piezoelectricity is one of its most important properties (Ahmed et al. 2022; Wu et al. 2022; Salimi and Yousefi 2003). This property converts mechanical energy into electrical energy and vice versa (He et al. 2021). This and other characteristics make PVDF suitable for applications, such as filtration, tissue engineering, monitoring, solar devices, battery electrolytes, and molecular separation (Wu et al. 2022; Saxena and Shukla 2021). PVDF occurs in five different phases. This polymorphism can also be observed when the material is exposed to high electrical charge, stretching, specific temperatures, and other processes (Zhou et al. 2023). The three most common PVDF phases can be seen in Fig. 1.

Given the piezoelectric properties of natural bone, materials with this property find applications as biomaterials due to their ability to generate bioelectric signals through the direct or converse piezoelectric effect (Sun et al. 2024; Saxena and Shukla 2021; Carter et al. 2021). Piezoelectric biomaterials are advantageous as they offer a wider range of materials for specific applications and eliminate complications associated with donor tissue, such as those encountered with autograft and allograft implants (Carter et al. 2021; Kathera et al. 2025; Choudhury et al. 2025). Considering these aforementioned advantages, as well as the biocompatibility of PVDF, this polymer can be used as a biomaterial for different applications (Concha et al. 2024; Carter et al. 2021; Szewczyk et al. 2019). As a biomaterial, PVDF in its β -phase form

is typically used for suture materials and surgical meshes (Wu et al. 2022; Petersmann et al. 2020).

The production of PVDF fibres is crucial for their use in biomaterials (Sun et al. 2024; Elnabawy et al. 2023; Concha et al. 2024). Similar to other materials, such as polylactic acid (PLLA) and polycaprolactone (PCL), PVDF requires precise parameter control during the spinning process to achieve a significant β -phase percentage, high fibre production, and optimal performance as a biomaterial (Elnabawy et al. 2023). However, the production yield of PVDF fibres can sometimes be insufficient, necessitating additional manufacturing batches.

In this work, aiming to increase both fibre productivity and PVDF biocompatibility, a solution comprising Ca(NO₃)₂·4H₂O and triethyl phosphate (TEP) ((C₂H₅)₃PO₄) as sources of calcium and phosphorus was used. This solution was mixed with dimethylformamide (DMF), acetone (ACE) and PVDF and processed via electroblowing to produce fibres with ceramic fillers. Considering that the DMF and the ACE, two solvents highly used to spin PVDF, will evaporate during processing, the biocompatibility of the final fibre can be ensured in this case, as the PVDF has already been extensively reported in the literature for its use as a biomaterial (Concha et al. 2024; Ahmed et al. 2022; Wu et al. 2022; Barski et al. 2017; Mullaveettil et al. 2021; Correa Braga et al. 2007; Cheng et al. 2020; Li et al. 2009; Abd El-Aziz and Afifi 2024).

The HAp precursor solution was added in different percentages to the PVDF solution to investigate the effects on fibre morphology, production rate, and β -phase percentage. This approach aimed to create a

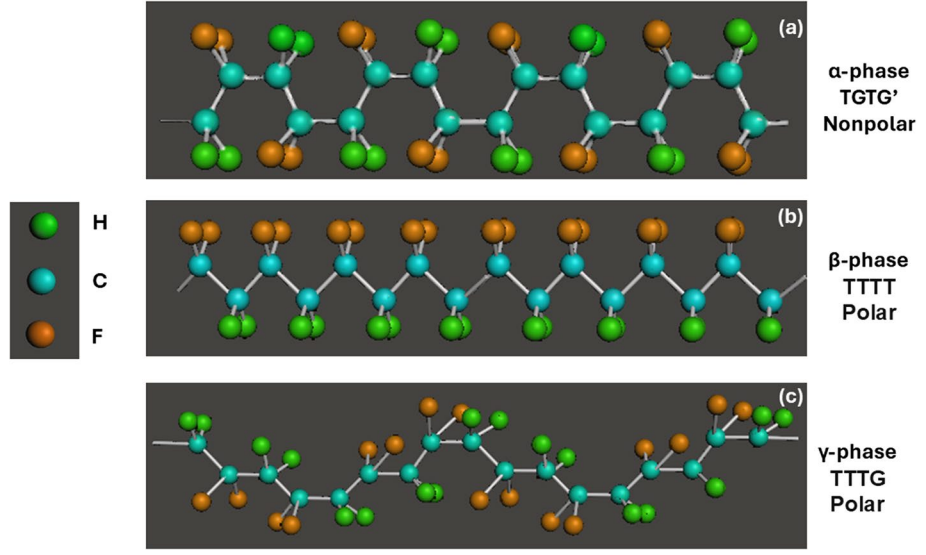


Fig. 1 PVDF: **a** α -phase, **b** β -phase, and **c** γ -phase

more stable composite fibrous biomaterial by combining the HAp precursor solution with the electroblowing technique. Given the increased risk of clogging when using powder-based fillers, employing the desired bioceramic derived from precursor solutions presents a promising alternative. This approach enhances spinning control by enabling more precise regulation of filler size through controlled nucleation and growth from calcium and phosphate sources, which are already used in the literature to form hydroxyapatite (Holopainen and Ritala 2016; Mokhtari et al. 2025).

Material and methods

First, a HAp precursor solution was prepared with magnetic stirring at room temperature with 9.27 g of Ca(NO₃)₂·4H₂O from Merck, 4 mL TEP (99%) from ABCR Gute Chemie, and 10 mL of absolute EtOH from VWR Chemicals (Pasuri et al. 2015). A second solution was prepared with PVDF acquired from

Solvay Rhodia (Brazil) dissolved in DMF and acetone (ACE) (Zhou et al. 2023).

The PVDF powder (PVDF Solvay, Brazil) was dissolved in 80% DMF from Merck and 20% ACE from VWR Chemicals, ensuring a 14% polymer concentration in the solution, solvents selected for their extensive use in research involving PVDF fibres (Al Rai et al. 2020; Chacko and Raneesh 2023; Martins et al. 2014; Tandon and Cartmell 2019). The HAp precursor solution was added in proportions of 5% and 10% (v/v) to the 14% PVDF solution. The selection of these proportions took into account the influence of the lower viscosity of the precursor solution, which could significantly impact the reliability of the polymer solution due to the higher viscosity expected in the latter, and was also guided by relevant literature references (Tandon and Cartmell 2019; Kim and Fan 2021). This final solution was stirred for 1 h at 65 °C to obtain a final homogeneous solution. Figure 2 shows the steps involved in preparing the final solution, with precursors dispersed in a 14% PVDF polymeric solution.

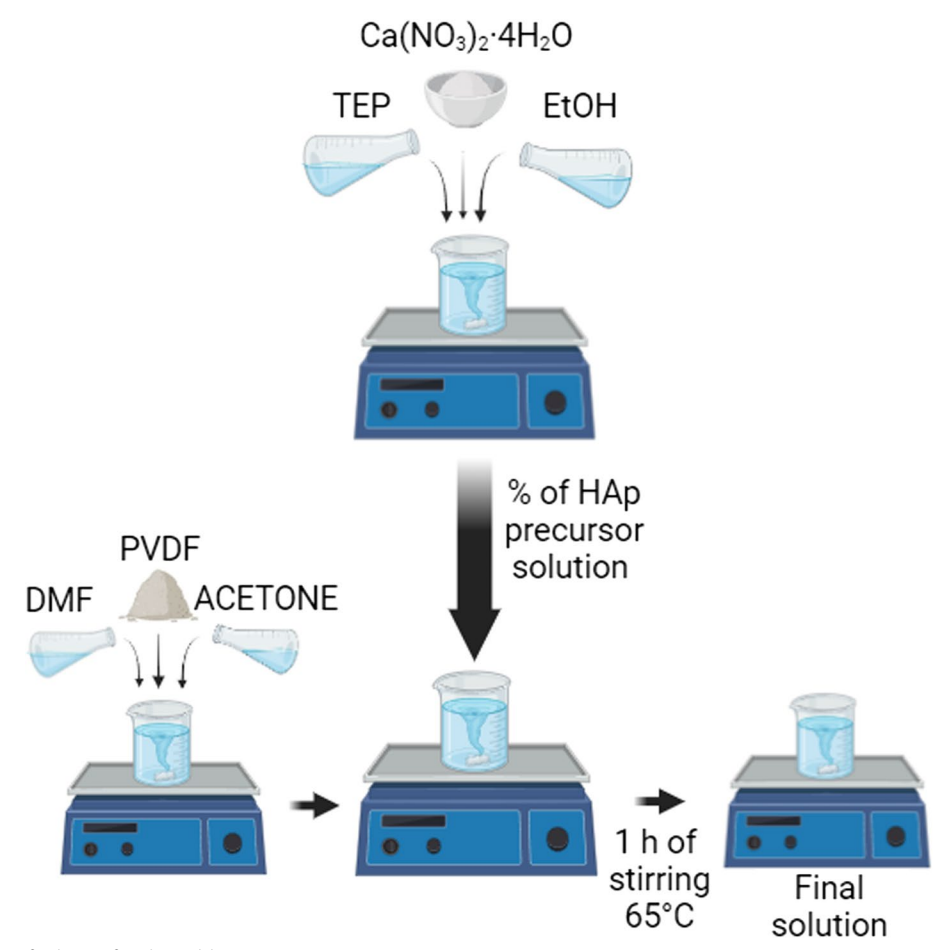


Fig. 2 Preparation of solution for electroblowing

After stirring, the solution was placed in a 12 mL syringe (HSW) with a 21G (0.21 mm inner diameter) needle. For electroblowing, the solution was delivered by a syringe pump (KDS Legato $^{\rm TM}$ 101). All the electroblowing parameters can be found in Table 1, while an illustration of the device can be seen in Fig. 3.

The parameters were maintained across the three types of fibre preparation: PVDF fibres without HAp precursors (PVDF), PVDF fibres with 5% HAp precursors (PVDF/HAp Precursors 5%), and PVDF fibres with 10% HAp precursors (PVDF/HAp Precursors 10%). As illustrated in Fig. 3, the device consists of two collectors, the side collector and the back collector, each located at different distances from the needle. This large area setup ensures effective collection of fibres during the spinning process.

After the spinning, the samples were characterised by a variety of techniques: X-ray diffraction (XRD) using a Rigaku Ultima IV X-ray diffractometer; scanning electron microscopy (SEM, FESEM, Hitachi S-4800) with

Table 1 Parameters for electroblowing

System parameters	
Polymer concentration (wt%)	14%
Solvent ratio (DMF/acetone)	80/20
Temperature in the box, T (°C)	~ 22,1
Voltage, V (kV)	20
Solution flow rate (mL/h)	6
Primary airflow (NL/min)	30
Secondary airflow (NL/min)	40
Temperature of stirring (°C)	65
Humidity (%)	35±5

a 4 nm layer of Au/Pd deposited by sputtering before analysis, preventing charging of the samples and producing better quality images; Raman spectroscopy (Horiba, LabRam HR Evolution); Fourier-transform infrared FTIR spectroscopy (FTIR iS10 Spectrometer, Nicolet), mechanical tensile (TA Instruments DMA Q800 V21.3 Build 96), transmission electron microscopy (TEM) (Thermo Fisher/FEI Titan Cubed Themis). Viscosity analysis was also performed using a TA Instruments DHR-2 rheometer with a 50-mm parallel plate geometry at room temperature, considering the solution used for the spinning process. These analysis methods were chosen to evaluate the impact of the precursors on phase content, morphology, elemental composition, and compound formation in fibres. The ImageJ software (Rasband 2018) was used to determine the average fibre diameter based on the measurement of 100 individual fibres from different areas of the SEM images. The β-phase fraction was determined using Eq. 1, which is based on Beer-Lambert's law, as explained by Gregorio and Cestari (Grecorio and Cestari 1994):

$$F(\beta) = \frac{A_{\beta}}{\left(\frac{K_{\beta}}{K_{\alpha}}\right)A_{\alpha} + A_{\beta}} \tag{1}$$

where $F(\beta)$ represents the β -phase fraction; A_{α} and A_{β} are the FTIR absorbance at around 763 and 840 cm⁻¹, respectively; and K_{α} and K_{β} are the absorption coefficients, which are 6.1×10^4 and 7.7×10^4 cm²/mol, respectively (Grecorio and Cestari 1994; Koroglu et al. 2021; Ma et al. 2017).

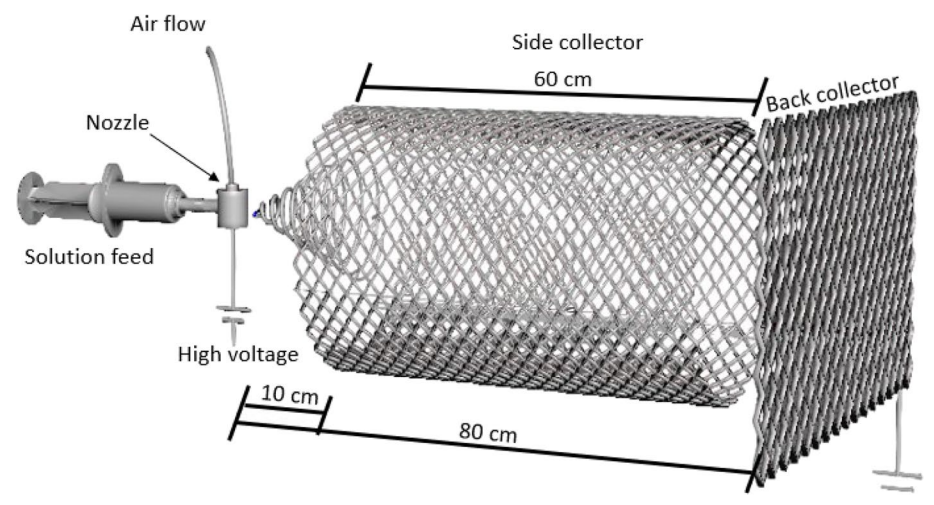


Fig. 3 A schematic of the experimental setup of the electroblowing technique

Results and discussions

The initial preparation of fibres involved controlling the electroblowing parameters without adding precursors (PVDF). In the case of the other samples (PVDF/HAp Precursors 5% and PVDF/HAp Precursors 10%), the calcium and phosphorous precursors were added to just change the morphology of the fibres. However, the HAp precursors were also found to increase the area over which the fibres deposited on the collector (Fig. 4).

Figure 4a and b show the fibre distribution on the collector when the spinning was done with the polymeric solution without HAp precursors (PVDF). Figure 4b highlights preferential fibre deposition on the upper left side of the back collector. This behaviour could be attributed to the strong influence of the airflow directing the fibres during deposition and the phase conformation of the polymer, which exhibits less response to the electrical field in its non-polar α -phase compared to the β-phase which presents the highest dipole moment (Koroglu et al. 2021). The addition of the HAp precursors appears to enhance the conductivity of the solution, resulting in more uniform fibre distribution on the collectors, as shown in Fig. 4c for the PVDF/HAp Precursors 5% sample. Ultimately, a significant amount of material was observed, as depicted in Fig. 4d where the fibre mat from the collectors has been folded multiple times over a silicon wafer with a diameter of 150 mm.

Additionally, it was observed that the addition of HAp precursors facilitated the detachment of fibres at the collectors, resulting in a reduction in the amount of material lost due to decreased sticking. This effect can also be influenced by the high potential applied during the process, which contributes to phase changes in PVDF. Such changes are induced by the high electrical potential during poling and the presence of acetone mixed with DMF (Debili et al. 2020; Singh et al. 2021).

X-ray diffraction

Phase analysis was conducted using XRD to determine if the addition of HAp precursors influenced the phases present in the materials. Figure 5 shows the XRD patterns of the three samples, showing both the α and β phases. For the PVDF sample without the HAp precursors (PVDF), the α -phase peaks at 18.4° and 19.9° and the β -phase peak at 20.6° are clearly visible (Cheng et al. 2020; Debili et al. 2020; Vasic et al. 2021).

When the HAp precursors were incorporated, additional peaks (36.6° and 41.2°) corresponding to the hydroxyapatite appeared alongside the peaks related to the α -phase and β -phase (Cheng et al. 2020; Debili et al. 2020; Vasic et al. 2021). The peaks associated with HAp

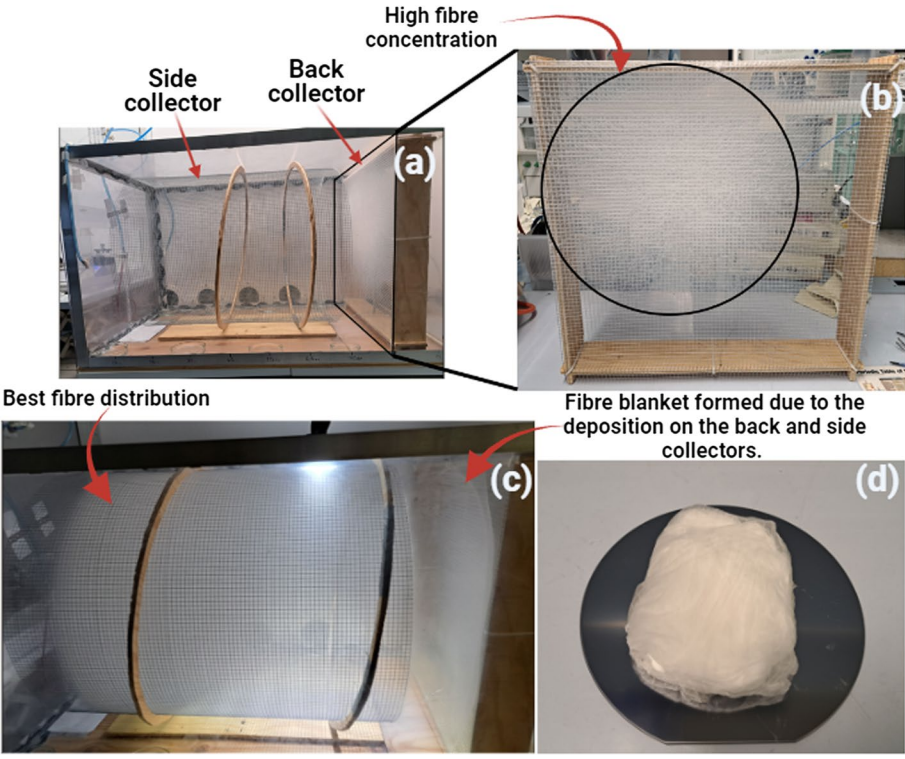


Fig. 4 Images showing a and b different fibre deposition of PVDF and c and d PVDF fibre obtained with HAp precursors

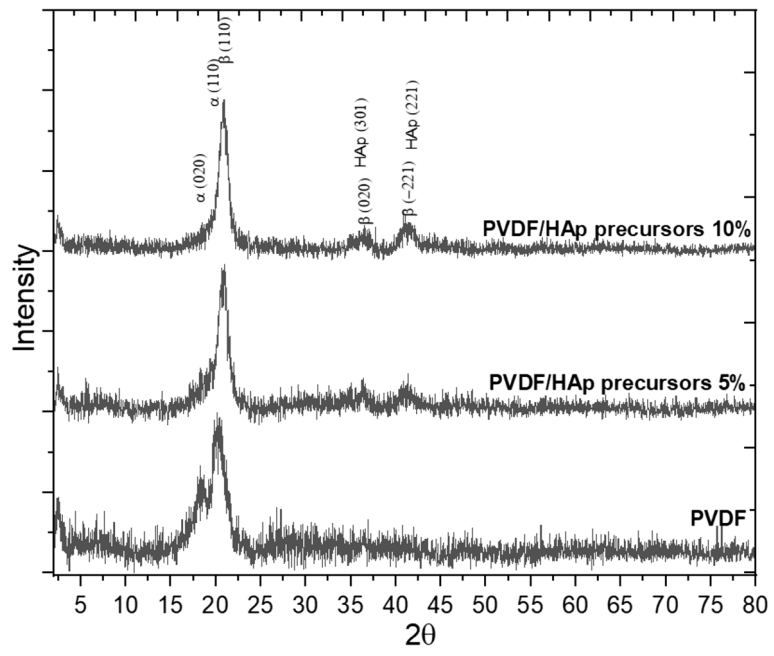


Fig. 5 XRD patterns of PVDF with and without additions of 5% and 10% HAp precursors

are located at 36.4° and 42.03° (Bakan et al. 2013; Merzougui et al. 2022). These two peaks are easily observed in the samples with precursors, indicating the successful integration of ceramic fillers into the final fibres. These peaks are absent when there are no precursors on the PVDF fibres.

The precursor solution also influences the PVDF β -phase intensity, which increases when the precursors are added (36.4° and 42.03°). This interaction between HAp precursors and PVDF α -phase considering their electrical charges suggests that the presence of precursors results in an α/β -phase conversion, a phenomenon commonly observed in this polymer because the β -phase is more stable with the high potential environment lending to the increase of the polarization effect and making more easily polar phase (β -phase) occurrence (Concha et al. 2024; Ahmed et al. 2022).

The transition of the α -phase to the β -phase supports the idea of enhanced electrical properties due to the change from the non-polar (α -phase) phase to the polar phase (β -phase) (Ma et al. 2017). This phase transition influences the distribution of fibres over a larger area of the collectors, as observed in Fig. 4c.

SEM

SEM analysis was performed to examine the morphology of the fibres and the effect of increasing the HAp precursor content. According to Fig. 6, the fibre diameter increased with higher precursor concentration. While

it is known that the percentage of solvent influences fibre diameter, the solvent percentage remained constant across all samples (Yin et al. 2022). Therefore, the observed changes in fibre diameter and bead formation are attributed to the addition of HAp precursors.

Figure 6a shows the effect on the fibres obtained during spinning via electroblowing. Beads with an average diameter of 2.4 μm are seen in the PVDF sample (Fig. 6a and d). In Fig. 6b and c, a significant reduction in bead formation is evident, suggesting an influence of the precursors on this aspect of fibre morphology. Figure 6d, e and f show the fibre morphology at higher magnification for the same three samples, highlighting a reduction in the packing density of fibres, which is linked to an improved fibre distribution in the samples containing HAp precursors (PVDF/HAp Precursors 5% and PVDF/HAp Precursors 10%).

Another effect of the precursors is that as their percentage increases, the diameter of the fibres also increases. In the sample with no precursors, the average diameter was 0.2 μm (Fig. 7a), which increased to 1.1 μm for the sample with 5% precursors (Fig.7b) and 1.6 μm in the sample with 10% precursors (Fig. 7c). Analysis of these samples indicates a Gaussian distribution of fibre diameters when HAp precursors are used. This can be attributed to the more homogeneous distribution of fibres across the collectors.

Considering this effect, it is possible to correlate fibre diameter with cellular adhesion, proliferation, and

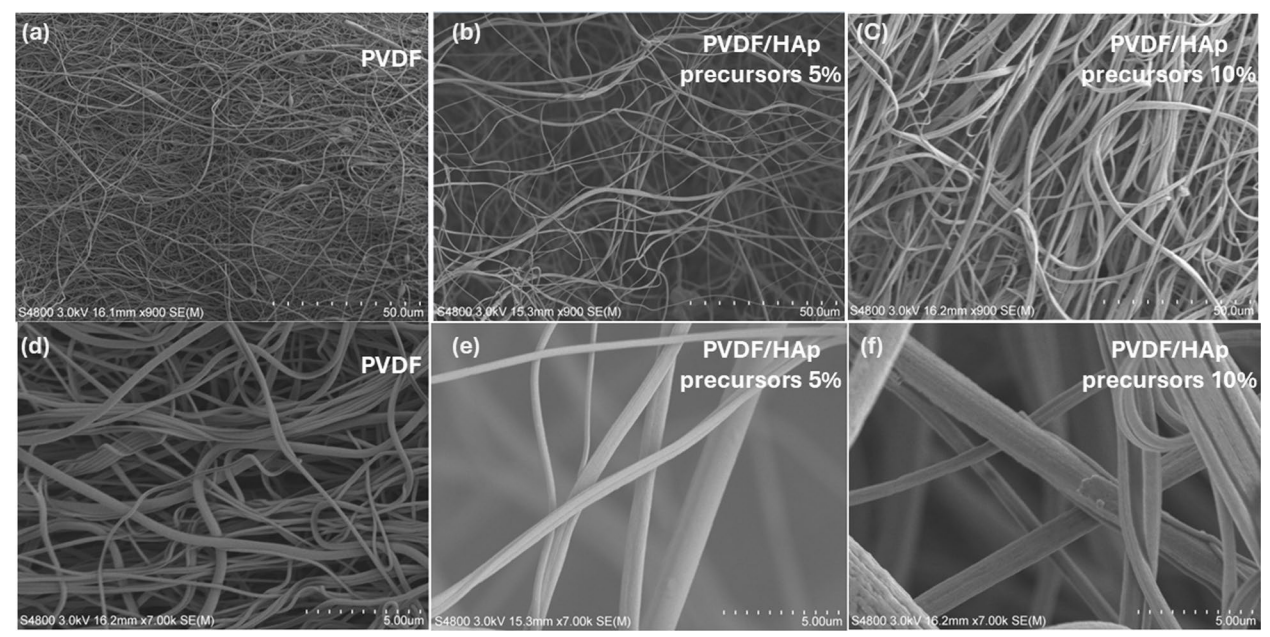


Fig. 6 SEM images of **a** PVDF 900 ×, **b** PVDF/HAp Precursors 5% 900 ×, **c** PVDF/HAp Precursors 10% 900 ×, **d** PVDF 7000 ×, **e** PVDF/HAp Precursors 5% 7000 ×, **f** PVDF/HAp Precursors 10% 7000 ×

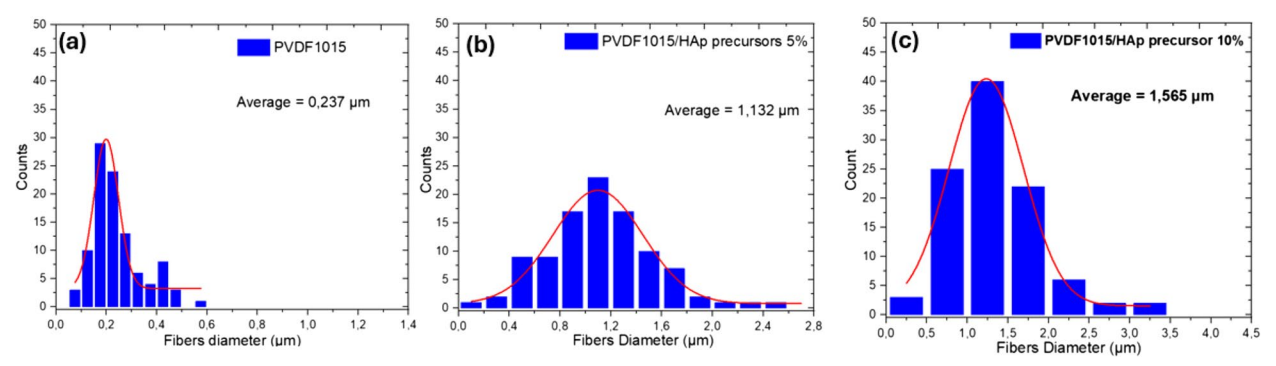


Fig. 7 a Fibre diameter distribution of PVDF, **b** fibre diameter distribution of PVDF/HAp precursors 5%, and **c** fibre diameter distribution of PVDF/HAp precursors 10%

differentiation; an increase in fibre diameter alters the surface properties, potentially hindering cell–composite interactions (Chen et al. 2007; Tandon et al. 2019). However, although larger fibre diameters may reduce cell adhesion, the presence of hydroxyapatite (HAp) counteracts this effect by enhancing cell–material interactions, due to the well-established high biocompatibility of this ceramic (Chen et al. 2007; Tandon et al. 2019; Gittings et al. 2009; Zima 2018; Yuwono and Siswanto 2023; Rodriguez et al. 2016).

The observed morphological changes suggest that adjusting the amount of HAp precursors can fine-tune the fibre parameters, enhancing the applicability of the final product for biomaterial studies considering the changes in the available surface area and therefore the interaction of the biomaterial with the environment (Zhang et al. 2024; Barbosa et al. 2022). The few visible HAp particles, due to nucleation and grain growth, suggest a good distribution of the precursor solution within the polymer matrix.

FTIR

FTIR is commonly used as a complementary technique to verify PVDF phase formation and the presence of other compounds resulting from the interaction between the polymeric solution and the precursor solution containing TEP, Ca(NO₃)₂·4H₂O, and EtOH. Figure 8 shows the spectra of the three samples,

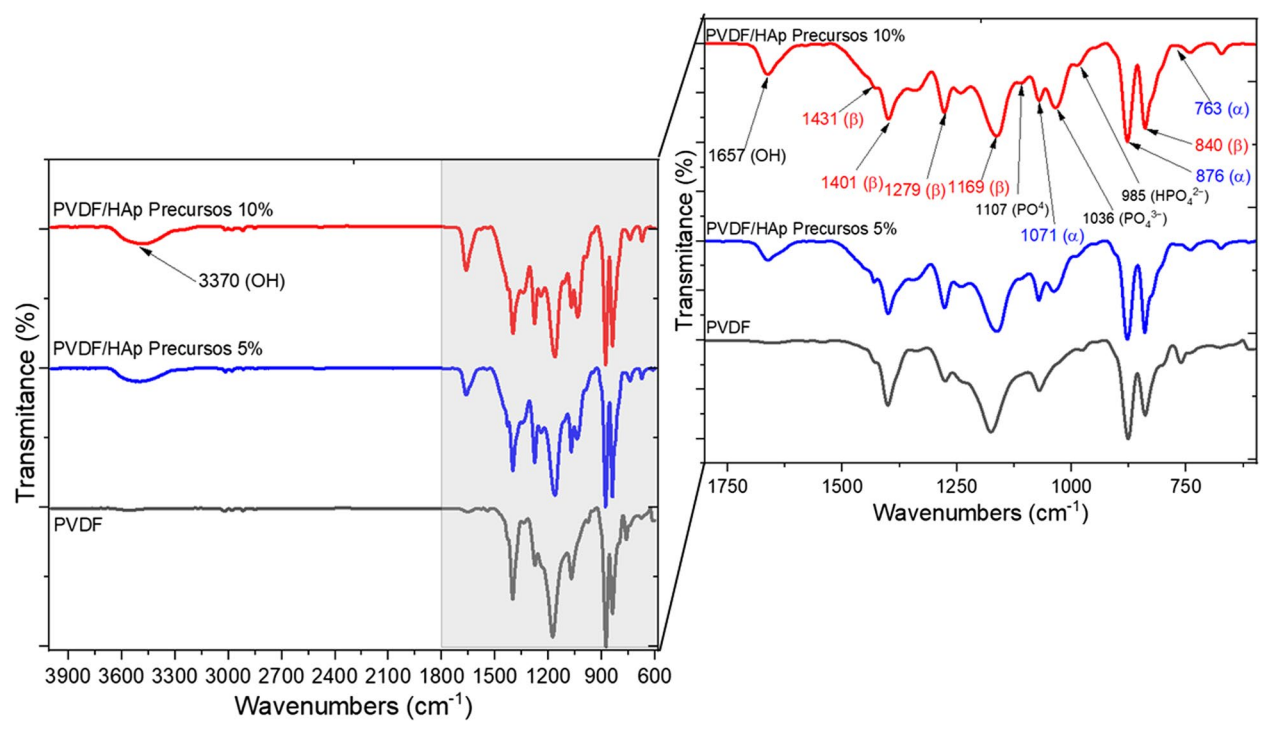


Fig. 8 FTIR spectra of PVDF, PVDF/HAp Precursors 5%, and PVDF/HAp Precursors 10%

highlighting the compounds and suggesting phase transitions. An increase in peak intensity is observed for the samples containing HAp precursors.

The peaks representing the α -phase are easily observed at wavelengths of 763, 876, and 1071 cm⁻¹ (Wu et al. 2022; Cheng et al. 2020; Yoon et al. 2024), while the peaks for the β -phase are at 840, 1169, 1279, 1401 (associated with CH₂ wagging mode), and 1431 cm⁻¹ (Cheng et al. 2020; Debili et al. 2020; Singh et al. 2021; Pradhan et al. 2023). Peaks related to the HAp are observed at 985 (related to the P-O stretching mode in PO₄), 1036 (PO₄³⁻), 1107, and 1657 cm⁻¹ (OH) (Bakan et al. 2013; Costa et al. 2024; Goh et al. 2021; Mondal et al. 2014).

Phase percentage analysis was carried out using Eq. 1. When only the α and β phases are present on the polymeric matrix, it is possible to use this equation and estimate the amount of these two phases (Cai et al. 2017).

Figure 9 shows the β -phase percentage according to Eq. 1 for the three samples. Considering the peaks at 763 and 840 cm⁻¹ for the two samples, it was concluded that the β -phase remained at around 70.93% with significant changes when compared with the PVDF and PVDF/HAp Precursors 5%. For the third case, PVDF/HAp Precursors 10%, a minor increase in the amount of the β -phase was observed.

RAMAN

Figure 10 shows the results from Raman spectroscopy analysis. An increase in peak intensity is observed at 1044 cm⁻¹ when the HAp precursors are added (Rodrigues et al. 2020). The peaks at 795, 880, 1430, 2977, and 3015 cm⁻¹ indicate the presence of α -phase, while the peaks at 510, 840, and 1279 cm⁻¹ represent the β -phase (Chipara et al. 2020). This analysis indicates that HAp precursors increase the presence of the β -phase, particularly for the 510, 840, and 1279 cm⁻¹ peaks. The α -phase peaks at 795 and 880 cm⁻¹ show a reduced intensity with the addition of the HAp precursors, supporting the findings from the FTIR analyses.

The increase in the β -phase may be linked to the higher percentage of HAp precursors, which changes the polymer conformation towards the β -phase. This suggests that a threshold amount of HAp precursors is needed to increase the β -phase content. The final analysis suggests that even with the transitional behaviour of the α and β phases, even a minor increase in the β -phase percentage requires at least 10% of HAp precursors (Fig. 9).

Viscosity

Viscosity analyses were conducted to evaluate the behaviour of polymer solutions prepared for electroblowing, in the absence and presence of HAp precursor solutions. These analyses enabled the assessment of the influence

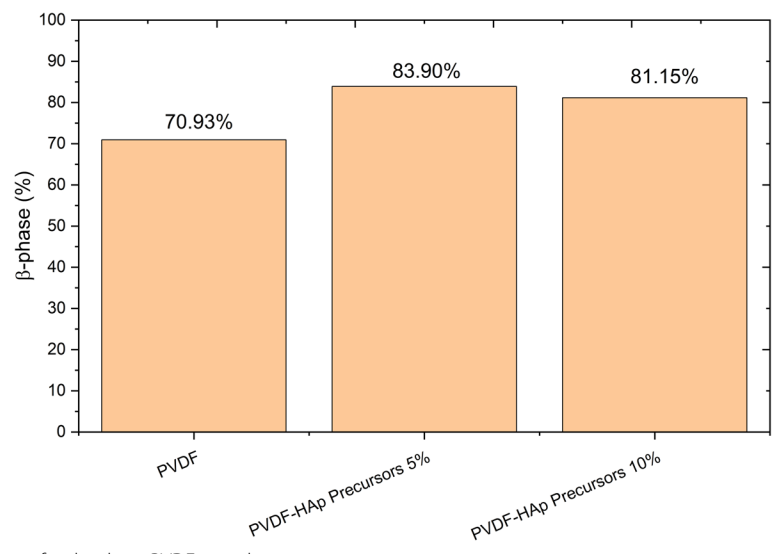


Fig. 9 The β -phase percentage for the three PVDF samples

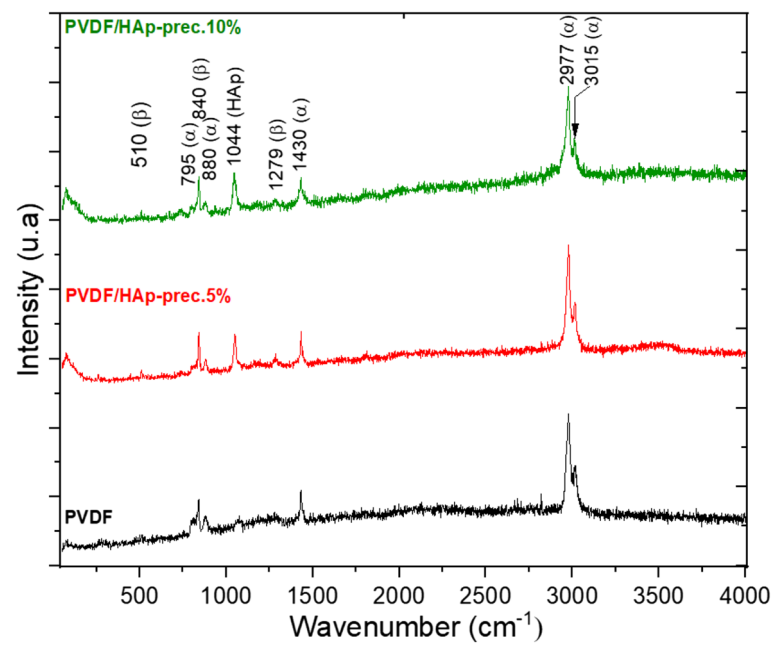


Fig. 10 Raman spectra of PVDF and PVDF/HAp precursor fibres

of precursor addition, at two different concentrations, on the viscosity of the solutions loaded into the syringe during fibre spinning. Figure 11 shows the relationship between viscosity and shear rate for the pure PVDF solution, PVDF with 5% HAp precursor, and PVDF with 10% HAp precursor.

As expected, the lowest viscosity was observed for the PVDF solution without precursor addition (Tandon and Cartmell 2019). However, the anticipated trend of increasing viscosity with higher precursor concentrations was not observed. The solution containing 5% precursor exhibited the highest viscosity, which changed the trending interpretation of the precursor concentration's effect on the overall viscosity of the polymer solution.

Although a linear relationship was not observed, the presence of precursors appears to increase the viscosity of the spinning solution due to their interaction with the polymer. This effect may be associated with the surface area of the precursor particles, as a larger surface area promotes greater particle/polymer interaction (Yang

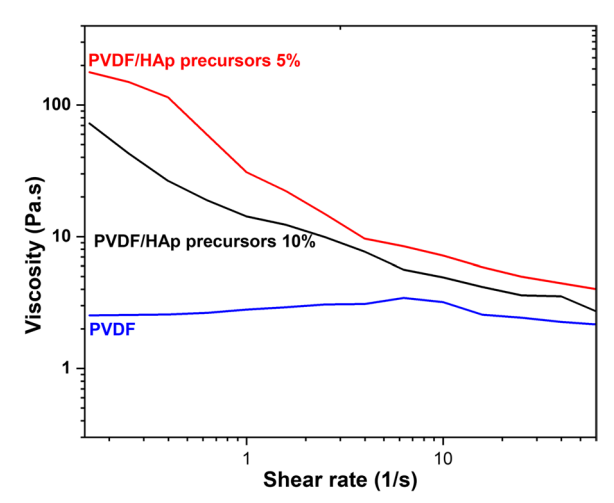


Fig. 11 Viscosity curves of PVDF and PVDF/HAp precursor fibres

et al. 2018). Thus, even small amounts of precursor solution have a significant impact on the viscosity of polymer solutions used in the electroblowing process (Yang et al. 2018; Cui et al. 2023). This observation highlights the need to define appropriate limits for both the amount

of precursor solution to be added and the viscosity of the polymer solution prior to mixing, in order to avoid clogging during fibre spinning considering the nucleation and growth of the HAp particles during the stirring in different sizes and the formation of clusters.

TEM

Regarding the TEM analyses, it was possible to investigate the distribution of HAp particles following the nucleation and growth processes from the added precursors (Goh et al. 2021). Additionally, the absence of such particles in the PVDF samples without precursor addition was confirmed.

Figure 12 presents the TEM images of the three samples studied. In Fig. 12a and d, as expected, no HAp particles were observed in the cross-sectional or outer regions of the pure PVDF fibres as expected. This condition was maintained even in fibres with diameters larger than the average. In Fig. 12b and e, corresponding to PVDF fibres containing 5% HAp precursors, particles with an average diameter of approximately 20 nm were observed, and the visualization of a relative homogeneous distribution was possible through images.

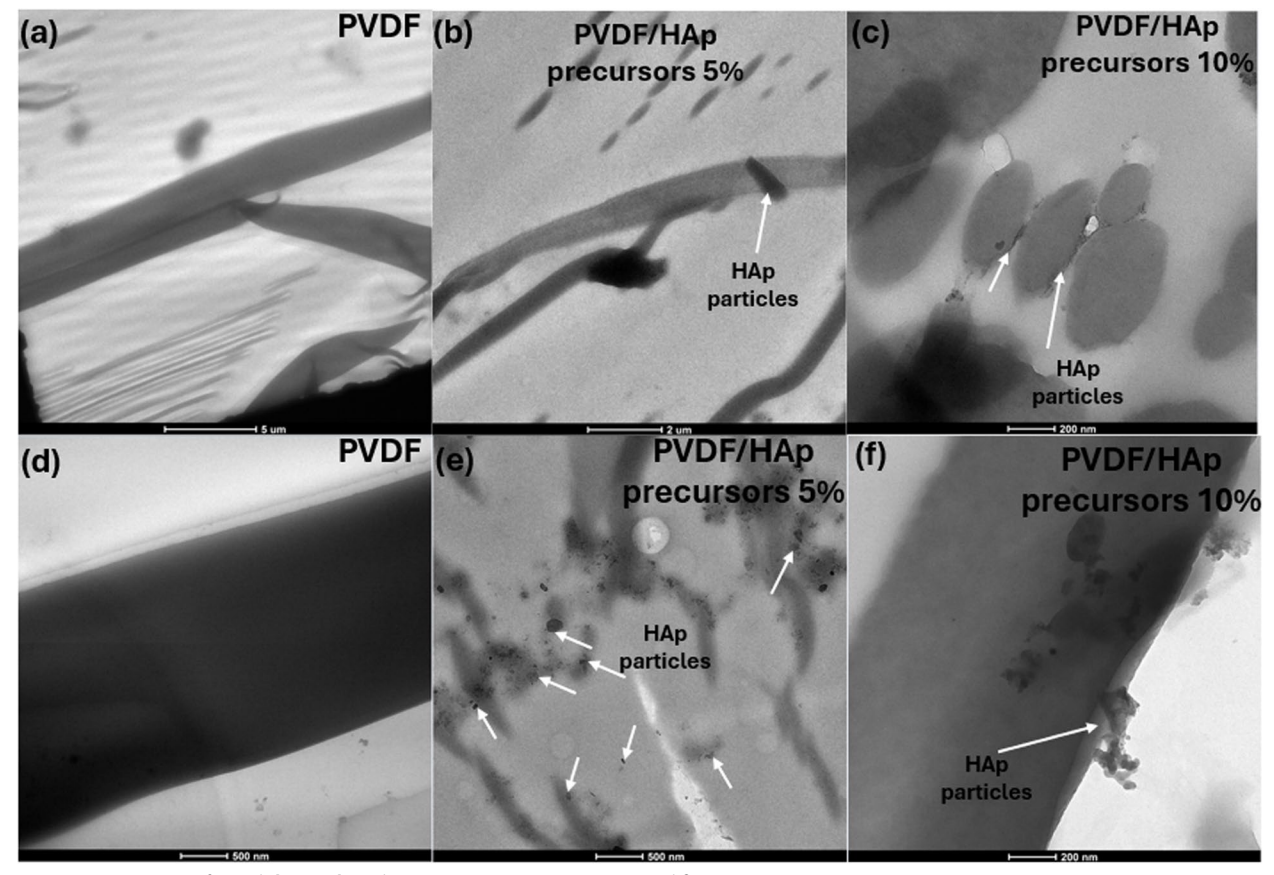


Fig. 12 TEM images of **a** and **d** PVDF, **b** and **e** PVDF/HAp Precursors 5%, **c** and **f** PVDF/HAp Precursors 10%

Figure 12c and f show the images of PVDF fibres with 10% HAp precursors, where particles with an average diameter of approximately 34.51 nm were detected. In this case, particle concentration was predominantly observed on the outer surfaces of the fibres, with no significant indication of particle formation inside the fibres. This behaviour may be attributed to the dispersion of a considerable amount of material during processing, leading to particle aggregation on the fibre surface.

Mechanical testing

Tensile tests were conducted to evaluate the effects of precursor solution addition on the mechanical properties of the HAp-containing samples, as well as to assess the behaviour of samples without the presence of these materials. Figure 13 presents the corresponding stress—strain curves and reveals variations in the mechanical stability of the fibres under tensile loading.

The tensile analysis clearly demonstrated a direct influence of the precursor content on material brittleness, with increased precursor concentration leading to greater fragility. Considering that the presence of ceramic structures can act as stress concentration sites within the fibrous polymeric matrix, higher precursor proportions result in a reduction of tensile strength (Stratiotou Efstratiadis et al. 2024).

Conclusion

The production of PVDF fibres by electroblowing in a 14% polymeric solution, with and without HAp precursors, demonstrates a few phases conversion of this polymer from the α -phase to the β -phase. The precursor solution containing TEP, $Ca(NO_3)_2 \cdot 4H_2O$, and EtOH

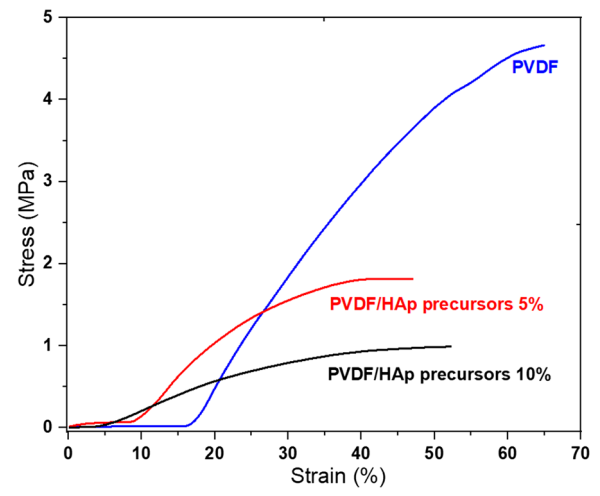


Fig. 13 Stress–strain curves of tensile testing of fibres of PVDF and PVDF with HAp precursors

significantly enhanced fibre distribution, leading to deposition across all collectors rather than just at a single region on the electroblowing device. The addition of 5% and 10% v/v precursor solution to the polymeric solution led to increased fibre diameter and improved homogeneity, with diameters increasing from 0.237 μm without precursors to 1.565 μm with 10% of HAp precursors.

The precursor solution containing TEP, $Ca(NO_3)_2 \cdot 4H_2O$, and EtOH effectively improved the spinnability of PVDF, changing the morphology and phase composition of the polymeric matrix. This final solution of PVDF dissolved in DMF, with the addition of the precursor solution, proves to be a promising method for promoting fibre production for biomedical applications. This is attributed to the increased presence of the β -phase and the expected enhancement in biocompatibility resulting from the incorporation of HAp precursors into a biomaterial with potential for extensive biomedical applications.

Moreover, TEM analyses revealed an internal distribution of ceramic particles within the fibres at the 5% precursor concentration. However, with increasing HAp precursor content, a tendency for particle migration toward the outer regions of the fibres was observed. The tensile test results indicated a trend toward increased mechanical fragility of the fibres with higher precursor concentrations. Finally, the viscosity studies showed a tendency for viscosity to increase in the presence of precursor solution, although this effect did not follow a proportional relationship with the amount of precursor solution added.

Computational simulations can be employed in future studies to investigate the effects of interactions between the polymer solution and the precursor solution in the presence of β -phase, providing a deeper understanding of the influence of each factor. Furthermore, in vitro studies may expand the potential applications of this biomaterial across various biomedical fields.

Acknowledgements

The authors acknowledge with thanks the excellent technical support provided by Lauri Pettilä for the use of the device employed herein. This research used facilities of the Brazilian Nanotechnology National Laboratory (LNNano), part of the Brazilian Centre for Research in Energy and Materials (CNPEM), a private non-profit organization under the supervision of the Brazilian Ministry for Science, Technology, and Innovations (MCTI). The Electronic Microscopy staff is acknowledged for the assistance during the experiments (Proposal number 20251299).

Data and code availability

Data can be available if asked

Authors' contributions

Methodology, J.P. and M.R.; validation, J.P., M.R. and C.S.; investigation, J.P., M.R. and C.S.; writing—original draft preparation, J.P.; writing—review and editing, J.P., M.R. and C.S.; supervision, M.R. and C.S. All authors have read and agreed to the published version of the manuscript.

Funding

This work was funded by the Coordination for the Improvement of Higher Education Personnel—CAPES and National Council for Scientific and Technological Development—CNPq project number 311184/2022–7.

Data availability

The material can be provided if asked.

Declarations

Competing interests

The authors declare that they have no competing interests.

Author details

¹Department of Materials Engineering, São Carlos School of Engineering, University of São Paulo, São Carlos, SP, Brazil. ²Department of Chemistry, University of Helsinki, Helsinki, Finland. ³São Carlos Institute of Chemistry, University of São Paulo, São Carlos, SP, Brazil.

Received: 14 January 2025 Accepted: 23 June 2025 Published online: 16 October 2025

References

- Abd El-Aziz AM, Afifi M (2024) Influence the β-PVDF phase on structural and elastic properties of PVDF/PLZT composites. Materials Science and Engineering: B 301:. https://doi.org/10.1016/j.mseb.2023.117152
- Ahmed A, Jia Y, Deb H et al (2022) Ultra-sensitive all organic PVDF-TrFE E-spun nanofibers with enhanced β -phase for piezoelectric response. J Mater Sci: Mater Electron 33:3965–3981. https://doi.org/10.1007/s10854-021-07590-y
- Al Rai A, Stojanovska E, Fidan G et al (2020) Structure and performance of electroblown PVDF-based nanofibrous electret filters. Polym Eng Sci 60:1186–1193. https://doi.org/10.1002/pen.25372
- Bakan F, Laçin O, Sarac H (2013) A novel low temperature sol-gel synthesis process for thermally stable nano crystalline hydroxyapatite. Powder Technol 233:295–302. https://doi.org/10.1016/j.powtec.2012.08.030
- Barski D, Arndt C, Gerullis H et al (2017) Transvaginal PVDF-mesh for cystocele repair: a cohort study. Int J Surg 39:249–254. https://doi.org/10.1016/j.ijsu. 2017.02.006
- Bernard M, Jubeli E, Pungente MD, Yagoubi N (2018) Biocompatibility of polymer-based biomaterials and medical devices-regulations;: In vitro screening and risk-management. Biomater Sci 6:2025–2053
- Cai X, Lei T, Sun D, Lin L (2017) A critical analysis of the α , β and γ phases in poly(vinylidene fluoride) using FTIR. RSC Adv 7:15382–15389. https://doi.org/10.1039/c7ra01267e
- Carter A, Popowski K, Cheng K et al (2021) Enhancement of bone regeneration through the converse piezoelectric effect, a novel approach for applying mechanical stimulation. Bioelectricity 3:255. https://doi.org/10.1089/BIOE. 2021.0019
- Chacko SK, Raneesh B (2023) Dielectric, ferroelectric and magnetoelectric investigations of SrFe12O19-embedded PVDF-HFP nanocomposite fiber mats for flexible electronic applications. J Mater Sci 58:1158–1170. https://doi.org/10.1007/s10853-022-08093-9
- Chen M, Patra PK, Warner SB, Bhowmick S (2007) Role of fiber diameter in adhesion and proliferation of NIH 3T3 fibroblast on electrospun polycaprolactone scaffolds. Tissue Eng 13:579–587. https://doi.org/10.1089/ten. 2006.0205
- Cheng Y, Xu Y, Qian Y, et al (2020) 3D structured self-powered PVDF/PCL scaffolds for peripheral nerve regeneration. Nano Energy 69:. https://doi.org/ 10.1016/j.nanoen.2019.104411
- Chipara D, Kuncser V, Lozano K, et al (2020) Spectroscopic investigations on PVDF-Fe2O3 nanocomposites. J Appl Polym Sci 137:. https://doi.org/10.1002/app.48907
- Choudhury S, Das D, Roy S, Chowdhury AR (2025) Piezoelectric biomaterials for use in bone tissue engineering—a narrative review. J Biomed Mater Res B Appl Biomater 113, e35564

- Concha VOC, Timóteo L, Duarte LAN et al (2024) Properties, characterization and biomedical applications of polyvinylidene fluoride (PVDF): a review. J Mater Sci 59:14185–14204
- Correa Braga FJ, Rogero O, Couto AA, et al (2007) Characterization of PVDF/ HAP composites for medical applications
- Costa GM da, Everton GO, Amaral GO, et al (2024) Brushite/hydroxyapatite coatings on H2SO4 passivated 316LSS by electrodeposition: In vitro corrosion and anti-inflammatory activity. Surf Coat Technol 476:. https://doi.org/10.1016/j.surfcoat.2023.130304
- Cui Y, Sui Y, Wei P, et al (2023) Rationalizing the dependence of poly (vinylidene difluoride) (PVDF) rheological performance on the nanosilica. Nanomaterials 13:. https://doi.org/10.3390/nano13061096
- Debili S, Gasmi A, Bououdina M (2020) Synergistic effects of stretching/polarization temperature and electric field on phase transformation and piezoelectric properties of polyvinylidene fluoride nanofilms. Appl Phys A Mater Sci Process 126:. https://doi.org/10.1007/s00339-020-03492-8
- Demina TS, Bolbasov EN, Peshkova MA, et al (2022) Electrospinning vs. electro-assisted solution blow spinning for fabrication of fibrous scaffolds for tissue engineering. Polymers (Basel) 14:. https://doi.org/10.3390/polym14235254
- Elnabawy E, Sun D, Shearer N, Shyha I (2023) Electro-blown spinning: new insight into the effect of electric field and airflow hybridized forces on the production yield and characteristics of nanofiber membranes. Journal of Science: Advanced Materials and Devices 8. 100552
- Gittings JP, Bowen CR, Dent ACE et al (2009) Electrical characterization of hydroxyapatite-based bioceramics. Acta Biomater 5:743–754. https://doi.org/10.1016/j.actbio.2008.08.012
- Goh KW, Wong YH, Ramesh S et al (2021) Effect of pH on the properties of eggshell-derived hydroxyapatite bioceramic synthesized by wet chemical method assisted by microwave irradiation. Ceram Int 47:8879–8887. https://doi.org/10.1016/j.ceramint.2020.12.009
- Grecorio R, Cestari M (1994) Effect of crystallization temperature on the crystalline phase content and morphology of poly(vinylidene fluoride). J Polym Sci B Polym Phys 32:859–870. https://doi.org/10.1002/polb. 1994.090320509
- Harshal Gade SNGGCDHR (2021) Effect of electrospinning conditions on β-phase and surface charge potential of PVDF fibers. Polymer (Guildf) 1–13. https://doi.org/10.1016/j.polymer.2021.123902
- He Z, Rault F, Lewandowski M et al (2021) Electrospun PVDF nanofibers for piezoelectric applications: a review of the influence of electrospinning parameters on the β phase and crystallinity enhancement. Polymers (Basel) 13:1–23
- Holopainen J, Ritala M (2016) Rapid production of bioactive hydroxyapatite fibers via electroblowing. J Eur Ceram Soc 36:3219–3224. https://doi.org/10.1016/j.jeurceramsoc.2016.05.011
- Kathera CS, Cobandede Z, Titus K, et al (2025) Nanomaterial-based scaffolds for bone regeneration with piezoelectric properties. Nanomedicine 1–17. https://doi.org/10.1080/17435889.2025.2504320
- Kim M, Fan J (2021) Piezoelectric properties of three types of PVDF and ZnO nanofibrous composites. Advanced Fiber Materials 3:160–171. https://doi.org/10.1007/s42765-021-00068-w
- Koroglu L, Ayas E, Ay N (2021) 3D printing of polyvinylidene fluoride based piezoelectric nanocomposites: an overview. Macromol Mater Eng 306, 2100277
- Kujawa J, Boncel S, Al-Gharabli S, et al (2024) Current and future applications of PVDF-carbon nanomaterials in energy and sensing. Chemical Engineering Journal 492, 151856
- Li Q, Xu Z-L, Yu L-Y (2009) Effects of mixed solvents and PVDF types on performances of PVDF microporous membranes. J Appl Polym Sci 115:2277–2287. https://doi.org/10.1002/app.31324
- Li Y, Zhu J, Cheng H, et al (2021) Developments of advanced electrospinning techniques: a critical review. Adv Mater Technol 6, 2100410
- Luchese CL, Engel JB, Tessaro IC (2024) A review on the mercerization of natural fibers: parameters and effects. Korean J Chem Eng 41:571–587
- Ma B, Yang J, Sun Q et al (2017) Influence of cellulose/[Bmim]Cl solution on the properties of fabricated NIPS PVDF membranes. J Mater Sci 52:9946–9957. https://doi.org/10.1007/s10853-017-1150-2
- Martins P, Lopes AC, Lanceros-Mendez S (2014) Electroactive phases of poly(vinylidene fluoride): determination, processing and applications. Prog Polym Sci 39:683–706

- Merzougui M, Mezahi FZ, Dakhouche A et al (2022) Improvement of the reactivity of triethyl phosphate and structural behavior of hydroxyapatite versus the synthesis conditions by sol–gel route. Chem Pap 76:1045–1061. https://doi.org/10.1007/s11696-021-01938-8
- Mokhtari F, Samadi A, Rashed AO, et al (2025) Recent progress in electrospun polyvinylidene fluoride (PVDF)-based nanofibers for sustainable energy and environmental applications. Prog Mater Sci 148: 1–41
- Mondal S, Mondal A, Mandal N et al (2014) Physico-chemical characterization and biological response of Labeo rohita-derived hydroxyapatite scaffold. Bioprocess Biosyst Eng 37:1233–1240. https://doi.org/10.1007/s00449-013-1095-z
- Mullaveettil FN, Dauksevicius R, Wakjira Y (2021) Strength and elastic properties of 3D printed PVDF-based parts for lightweight biomedical applications. J Mech Behav Biomed Mater 120:. https://doi.org/10.1016/j.jmbbm.
- Paajanen J, Pettilä L, Lönnrot S, et al (2023) Electroblown titanium dioxide and titanium dioxide/silicon dioxide submicron fibers with and without titania nanorod layer for strontium(II) uptake. Chemical Engineering Journal Advances 13:. https://doi.org/10.1016/j.ceia.2022.100434
- Pasuri J, Holopainen J, Kokkonen H et al (2015) Osteoclasts in the interface with electrospun hydroxyapatite. Colloids Surf B Biointerfaces 135:774–783. https://doi.org/10.1016/j.colsurfb.2015.08.045
- Petersmann S, Spoerk M, Van De Steene W et al (2020) Mechanical properties of polymeric implant materials produced by extrusion-based additive manufacturing. J Mech Behav Biomed Mater 104:103611. https://doi.org/10.1016/j.jmbbm.2019.103611
- Pradhan SK, Kour P, Kumar A, et al (2023) Effect of ferroelectric filler nanoarchitectonics on the electrical and mechanical properties of the nanocomposite thick films of polyvinylidene fluoride and lanthanum-doped lead zirconate titanate in 0–3 connectivity. Appl Phys A Mater Sci Process 129:. https://doi.org/10.1007/s00339-023-07058-2
- Purushothaman SM, Tronco MF, Kottathodi B, et al (2023) A review on electrospun PVDF-based nanocomposites: recent trends and developments in energy harvesting and sensing applications. Polymer (Guildf) 283, 126179
- Rasband WS (2018) ImageJ. U. S. National Institutes of Health
- Rodrigues PJG, Elias CDMV, Viana BC et al (2020) Electrodeposition of bactericidal and bioactive nano-hydroxyapatite onto electrospun piezoelectric polyvinylidene fluoride scaffolds. J Mater Res 35:3265–3275. https://doi.org/10.1557/jmr.2020.302
- Rodriguez R, Rangel D, Fonseca G et al (2016) Piezoelectric properties of synthetic hydroxyapatite-based organic-inorganic hydrated materials. Results Phys 6:925–932. https://doi.org/10.1016/j.rinp.2016.11.005
- Salimi A, Yousefi AA (2003) FTIR studies of β -phase crystal formation in stretched PVDF films. Polym Test 22:699–704. https://doi.org/10.1016/S0142-9418(03)00003-5
- Saxena P, Shukla P (2021) A comprehensive review on fundamental properties and applications of poly(vinylidene fluoride) (PVDF). Adv Compos Hybrid Mater 4:8–76.
- Singh RK, Lye SW, Miao J (2021) Holistic investigation of the electrospinning parameters for high percentage of β-phase in PVDF nanofibers. Polymer (Guildf) 214:. https://doi.org/10.1016/j.polymer.2020.123366
- Stratiotou Efstratiadis V, Argyros A, Efthymiopoulos P, et al (2024) Utilization of silica filler as reinforcement material of polylactic acid (PLA) in 3D printing applications: thermal, rheological, and mechanical performance. Polymers (Basel) 16:. https://doi.org/10.3390/polym16101326
- Sun W, Gao C, Liu H et al (2024) Scaffold-based poly(vinylidene fluoride) and its copolymers: materials, fabrication methods, applications, and perspectives. ACS Biomater Sci Eng 10:2805–2826
- Szewczyk PK, Metwally S, Karbowniczek JE et al (2019) Surface-potential-controlled cell proliferation and collagen mineralization on electrospun polyvinylidene fluoride (PVDF) fiber scaffolds for bone regeneration. ACS Biomater Sci Eng 5:582–593. https://doi.org/10.1021/acsbiomaterials.
- Talita V Barbosa, Dernowsek JA, Tobar RJR, et al (2022) Fabrication, morphological, mechanical and biological performance of 3D printed poly(ε-caprolactone)/bioglass composite scaffolds for bone tissue engineering applications. 2d Mater 17: 0–38
- Tandon B, Kamble P, Olsson RT, et al (2019) Fabrication and characterisation of stimuli responsive piezoelectric PVDF and hydroxyapatite-filled PVDF fibrous membranes. Molecules 24:: https://doi.org/10.3390/molecules24101903, 1903

- Tandon BPKRTOJJB and, Cartmell SH (2019) Fabrication and characterisation of stimuli responsive piezoelectric PVDF and hydroxyapatite-filled PVDF fibrous membranes. Moleculas 20
- Vasic N, Steinmetz J, Görke M, et al (2021) Phase transitions of polarised pvdf films in a standard curing process for composites. Polymers (Basel) 13:. https://doi.org/10.3390/polym13223900
- Wang X, Sun F, Yin G, et al (2018) Tactile-sensing based on flexible PVDF nanofibers via electrospinning: a review. Sensors (Switzerland) 18, 330
- Wu L, Jin Z, Liu Y et al (2022) Recent advances in the preparation of PVDFbased piezoelectric materials. Nanotechnol Rev 11:1386–1407
- Yang B, Shi Y, Bin MJ et al (2018) Evaluation of rheological and thermal properties of polyvinylidene fluoride (PVDF)/graphene nanoplatelets (GNP) composites. Polym Test 67:122–135. https://doi.org/10.1016/j.polymertesting.2018.02.011
- Yin J-Y, Boaretti C, Lorenzetti A et al (2022). Effects of Solvent and Electrospinning Parameters on the Morphology and Piezoelectric Properties of PVDF Nanofibrous Membrane. https://doi.org/10.3390/nano
- Yoon SJ, Kim H, Jeong CK, Lee YK (2024) Highly stretchable and self-healing SEBS-PVDF composite films for enhanced dielectric elastomer generators. J Korean Ceram Soc. https://doi.org/10.1007/s43207-024-00369-x
- Yuwono LA, Siswanto SM et al (2023) Fabrication and characterization of hydroxyapatite-polycaprolactone-collagen bone scaffold by electrospun nanofiber. Int J Polym Mater Polym Biomater 72:1281–1293. https://doi.org/10.1080/00914037.2022.2097675
- Zhang M, Xu F, Cao J et al (2024) Research advances of nanomaterials for the acceleration of fracture healing. Bioact Mater 31:368–394
- Zhou J, Hou D, Cheng S, et al (2023) Recent advances in dispersion and alignment of fillers in PVDF-based composites for high-performance dielectric energy storage. Mater Today Energy 31, 101208
- Zima A (2018) Hydroxyapatite-chitosan based bioactive hybrid biomaterials with improved mechanical strength. Spectrochim Acta A Mol Biomol Spectrosc 193:175–184. https://doi.org/10.1016/j.saa.2017.12.008

Publisher's Note

Springer Nature remains neutral with regard to jurisdictional claims in published maps and institutional affiliations.